



KEK preprint 2002-31

Belle preprint 2002-15

Measurement of χ_{c2} Production in Two-Photon Collisions

Belle Collaboration

K. Abe⁸, K. Abe⁴⁰, R. Abe²⁸, T. Abe⁴¹, I. Adachi⁸, Byoung Sup Ahn¹⁵,
H. Aihara⁴², M. Akatsu²¹, Y. Asano⁴⁷, T. Aso⁴⁶, V. Aulchenko²,
T. Aushev¹², A. M. Bakich³⁷, Y. Ban³², E. Banas²⁶, A. Bay¹⁸,
P. K. Behera⁴⁸, A. Bondar², A. Bozek²⁶, M. Bračko^{19,13}, J. Brodzicka²⁶,
B. C. K. Casey⁷, P. Chang²⁵, Y. Chao²⁵, B. G. Cheon³⁶, R. Chistov¹²,
S.-K. Choi⁶, Y. Choi³⁶, M. Danilov¹², L. Y. Dong¹⁰, A. Drutskoy¹²,
S. Eidelman², V. Eiges¹², Y. Enari²¹, C. Fukunaga⁴⁴, N. Gabyshev⁸,
A. Garmash^{2,8}, T. Gershon⁸, R. Guo²³, F. Handa⁴¹, T. Hara³⁰, Y. Harada²⁸,
H. Hayashii²², M. Hazumi⁸, E. M. Heenan²⁰, I. Higuchi⁴¹, T. Hojo³⁰,
T. Hokuue²¹, Y. Hoshi⁴⁰, K. Hoshina⁴⁵, S. R. Hou²⁵, W.-S. Hou²⁵,
H.-C. Huang²⁵, T. Igaki²¹, Y. Igarashi⁸, K. Inami²¹, A. Ishikawa²¹, R. Itoh⁸,
M. Iwamoto³, H. Iwasaki⁸, Y. Iwasaki⁸, H. K. Jang³⁵, J. Kaneko⁴³,
J. H. Kang⁵¹, J. S. Kang¹⁵, P. Kapusta²⁶, S. U. Kataoka²², N. Katayama⁸,
H. Kawai³, Y. Kawakami²¹, N. Kawamura¹, T. Kawasaki²⁸, H. Kichimi⁸,
D. W. Kim³⁶, Heejong Kim⁵¹, H. J. Kim⁵¹, H. O. Kim³⁶, Hyunwoo Kim¹⁵,
S. K. Kim³⁵, T. H. Kim⁵¹, P. Krokovny², R. Kulasiri⁵, S. Kumar³¹,
A. Kuzmin², Y.-J. Kwon⁵¹, G. Leder¹¹, S. H. Lee³⁵, J. Li³⁴, D. Liventsev¹²,
R.-S. Lu²⁵, J. MacNaughton¹¹, G. Majumder³⁸, F. Mandl¹¹, S. Matsumoto⁴,
T. Matsumoto⁴⁴, K. Miyabayashi²², H. Miyake³⁰, H. Miyata²⁸,
G. R. Moloney²⁰, T. Mori⁴, T. Nagamine⁴¹, Y. Nagasaka⁹, E. Nakano²⁹,
M. Nakao⁸, J. W. Nam³⁶, Z. Natkaniec²⁶, K. Neichi⁴⁰, S. Nishida¹⁶,
O. Nitoh⁴⁵, S. Noguchi²², T. Nozaki⁸, S. Ogawa³⁹, F. Ohno⁴³, T. Ohshima²¹,
T. Okabe²¹, S. Okuno¹⁴, S. L. Olsen⁷, Y. Onuki²⁸, W. Ostrowicz²⁶,
H. Ozaki⁸, P. Pakhlov¹², H. Palka²⁶, C. W. Park¹⁵, H. Park¹⁷, K. S. Park³⁶,
L. S. Peak³⁷, J.-P. Perroud¹⁸, M. Peters⁷, L. E. Piilonen⁴⁹, N. Root²,
K. Rybicki²⁶, H. Sagawa⁸, S. Saitoh⁸, Y. Sakai⁸, M. Satapathy⁴⁸,
O. Schneider¹⁸, S. Schrenk⁵, C. Schwanda^{8,11}, S. Semenov¹², K. Senyo²¹,
R. Seuster⁷, M. E. Sevier²⁰, H. Shibuya³⁹, B. Shwartz², V. Sidorov²,
J. B. Singh³¹, S. Stanič^{47,*}, M. Starič¹³, A. Sugiyama²¹, K. Sumisawa⁸,

T. Sumiyoshi⁴⁴, S. Suzuki⁵⁰, S. K. Swain⁷, T. Takahashi²⁹, F. Takasaki⁸,
 K. Tamai⁸, N. Tamura²⁸, M. Tanaka⁸, G. N. Taylor²⁰, Y. Teramoto²⁹,
 S. Tokuda²¹, T. Tomura⁴², S. N. Tovey²⁰, T. Tsuboyama⁸, T. Tsukamoto⁸,
 S. Uehara⁸, K. Ueno²⁵, S. Uno⁸, S. E. Vahsen³³, G. Varner⁷, K. E. Varvell³⁷,
 C. C. Wang²⁵, C. H. Wang²⁴, J. G. Wang⁴⁹, M.-Z. Wang²⁵, Y. Watanabe⁴³,
 E. Won¹⁵, B. D. Yabsley⁴⁹, Y. Yamada⁸, A. Yamaguchi⁴¹, Y. Yamashita²⁷,
 M. Yamauchi⁸, H. Yanai²⁸, J. Yashima⁸, Y. Yuan¹⁰, Y. Yusa⁴¹, J. Zhang⁴⁷,
 Z. P. Zhang³⁴, V. Zhilich², and D. Žontar⁴⁷

¹*Aomori University, Aomori*

²*Budker Institute of Nuclear Physics, Novosibirsk*

³*Chiba University, Chiba*

⁴*Chuo University, Tokyo*

⁵*University of Cincinnati, Cincinnati OH*

⁶*Gyeongsang National University, Chinju*

⁷*University of Hawaii, Honolulu HI*

⁸*High Energy Accelerator Research Organization (KEK), Tsukuba*

⁹*Hiroshima Institute of Technology, Hiroshima*

¹⁰*Institute of High Energy Physics, Chinese Academy of Sciences, Beijing*

¹¹*Institute of High Energy Physics, Vienna*

¹²*Institute for Theoretical and Experimental Physics, Moscow*

¹³*J. Stefan Institute, Ljubljana*

¹⁴*Kanagawa University, Yokohama*

¹⁵*Korea University, Seoul*

¹⁶*Kyoto University, Kyoto*

¹⁷*Kyungpook National University, Taegu*

¹⁸*Institut de Physique des Hautes Énergies, Université de Lausanne, Lausanne*

¹⁹*University of Maribor, Maribor*

²⁰*University of Melbourne, Victoria*

²¹*Nagoya University, Nagoya*

²²*Nara Women's University, Nara*

²³*National Kaohsiung Normal University, Kaohsiung*

²⁴*National Lien-Ho Institute of Technology, Miao Li*

²⁵*National Taiwan University, Taipei*

²⁶*H. Niewodniczanski Institute of Nuclear Physics, Krakow*

²⁷*Nihon Dental College, Niigata*

²⁸*Niigata University, Niigata*

²⁹*Osaka City University, Osaka*

³⁰*Osaka University, Osaka*

³¹*Panjab University, Chandigarh*

³²*Peking University, Beijing*

³³*Princeton University, Princeton NJ*

³⁴*University of Science and Technology of China, Hefei*

³⁵*Seoul National University, Seoul*

³⁶*Sungkyunkwan University, Suwon*

³⁷*University of Sydney, Sydney NSW*

³⁸*Tata Institute of Fundamental Research, Bombay*

³⁹*Toho University, Funabashi*
⁴⁰*Tohoku Gakuin University, Tagajo*
⁴¹*Tohoku University, Sendai*
⁴²*University of Tokyo, Tokyo*
⁴³*Tokyo Institute of Technology, Tokyo*
⁴⁴*Tokyo Metropolitan University, Tokyo*
⁴⁵*Tokyo University of Agriculture and Technology, Tokyo*
⁴⁶*Toyama National College of Maritime Technology, Toyama*
⁴⁷*University of Tsukuba, Tsukuba*
⁴⁸*Utkal University, Bhubaneswer*
⁴⁹*Virginia Polytechnic Institute and State University, Blacksburg VA*
⁵⁰*Yokkaichi University, Yokkaichi*
⁵¹*Yonsei University, Seoul*
**on leave from Nova Gorica Polytechnic, Slovenia*

Abstract

The production of the χ_{c2} charmonium state in two-photon collisions has been measured with the Belle detector at the KEKB e^+e^- collider. A clear signal for $\chi_{c2} \rightarrow \gamma J/\psi$, $J/\psi \rightarrow \ell^+\ell^-$ is observed in a 32.6 fb^{-1} data sample accumulated at center-of-mass energies near 10.6 GeV, and the product of its two-photon decay width and branching fraction is determined to be $\Gamma_{\gamma\gamma}(\chi_{c2})\mathcal{B}(\chi_{c2} \rightarrow \gamma J/\psi)\mathcal{B}(J/\psi \rightarrow \ell^+\ell^-) = 13.5 \pm 1.3(stat.) \pm 1.1(syst.) \text{ eV}$.

Key words: two-photon collisions, charmonium, χ_{c2} , partial decay width
PACS: 13.20.Gd 13.40.Hq 13.65.+i 14.40.Gx

1 Introduction

The two-photon decay widths ($\Gamma_{\gamma\gamma}$) of the even charge-parity charmonium states provide valuable information for testing models describing the nature of heavy quarkonia. Various theoretical calculations describing the quark-antiquark system predict the value of $\Gamma_{\gamma\gamma}(\chi_{c2})$ to be within the range 0.2 – 0.8 keV [1]. A precise experimental determination of $\Gamma_{\gamma\gamma}(\chi_{c2})$ will provide a strong constraint on these models. The ratio of the two-gluon decay width to the two-photon decay width $\Gamma_{gg}(\chi_{c2})/\Gamma_{\gamma\gamma}(\chi_{c2})$ has been calculated within the framework of perturbative QCD with first-order correction [2] and the result gives $\Gamma_{\gamma\gamma}(\chi_{c2}) = 0.47 \pm 0.13$ keV.¹ A comparison of $\Gamma_{\gamma\gamma}(\chi_{c2})$ with the two-gluon width will provide a way to study the validity of perturbative QCD corrections for quarkonium decays.

Measurements of two-photon decay widths for charmonium states are difficult because of their small production cross section and small detection efficiencies. To date, several experiments have reported the observation of two-photon production of the χ_{c2} in the decay channel $\chi_{c2} \rightarrow \gamma J/\psi$, $J/\psi \rightarrow \ell^+\ell^-$, where $\ell = e$ or μ [5]. This channel is suitable for the experimental determination of $\Gamma_{\gamma\gamma}(\chi_{c2})$, since the decay branching fraction is known with a relatively small error, $\mathcal{B}(\chi_{c2} \rightarrow \gamma J/\psi)\mathcal{B}(J/\psi \rightarrow \ell^+\ell^-) = (1.59 \pm 0.13)\%$ for both lepton families [3]. However, the two-photon decay width results obtained from previous measurements with this process seem to be systematically larger than those from $p\bar{p} \rightarrow \chi_{c2} \rightarrow \gamma\gamma$ experiments [6]. Further studies with high statistics data samples are needed to clarify the situation.

Recently, the CLEO collaboration has reported a measurement of $\Gamma_{\gamma\gamma}(\chi_{c2})$ in the $\pi^+\pi^-\pi^+\pi^-$ final state [7]. Although the branching fraction of this decay mode, $\mathcal{B}(\chi_{c2} \rightarrow \pi^+\pi^-\pi^+\pi^-) = (1.2 \pm 0.5)\%$ [3], is comparable to that of the $\gamma J/\psi \rightarrow \ell^+\ell^-\gamma$ mode, its large error precludes a precise determination of $\Gamma_{\gamma\gamma}(\chi_{c2})$.

We have measured χ_{c2} production in two-photon processes using the decay channel $\chi_{c2} \rightarrow \gamma J/\psi$, $J/\psi \rightarrow \ell^+\ell^-$. The results are based on a 32.6 fb^{-1} data sample collected with the Belle detector.

¹ This value is derived from measurements [3] using the assumption that $\Gamma_{gg}(\chi_{c2})$ is given by $\Gamma(\chi_{c2} \rightarrow \text{hadrons}) - \Gamma(\chi_{c1} \rightarrow \text{hadrons})$ [4]. Here the strong coupling constant is set to be $\alpha_s(m_c) = 0.29 \pm 0.02$.

2 Experimental data and detector system

The experiment was performed with the Belle detector [8] at the asymmetric e^+e^- collider KEKB, where an 8.0 GeV e^- beam collides with a 3.5 GeV e^+ beam with a crossing angle of 22 mrad. We use a 29.6 fb^{-1} sample of data collected at the c.m. energy corresponding to the peak of the $\Upsilon(4S)$ resonance (10.58 GeV) and a 3.0 fb^{-1} sample collected 60 MeV below the peak.

The basic topology of events that we select is two tracks of opposite charge and a photon. The recoiling e^+ and e^- are not tagged in order to select quasi-real two-photon collisions with high efficiency. Events induced by highly virtual photons (i.e., photons with high- Q^2) are effectively rejected by a strict transverse momentum(p_t) requirement applied to the χ_{c2} daughter particles, as described in the following section.²

The charged track momenta are measured with a cylindrical drift chamber (CDC) located in a uniform 1.5 T magnetic field. Track trajectory coordinates near the collision point are provided by a silicon vertex detector (SVD). Photon detection and energy measurements are performed with a CsI electromagnetic calorimeter (ECL). The resolutions of track momentum and photon energy measurements are 0.4% for the leptons, which, for the signal process, have typical p_t values of 1.4 GeV/ c , and 2.0% for the photons, with typical energies of 0.4 GeV. The magnet return iron is instrumented to form the K_L and muon detector (KLM), which detects muon tracks and provides trigger signals.

The majority of the signal events are triggered by two-track triggers that require at least two tracks with transverse momenta larger than 0.2 GeV/ c detected in the CDC in coincidence with matching signals from TOF counters and trigger scintillation counters, isolated cluster or energy-sum signals from the ECL, or muon tracks in the KLM. A constraint on the opening angle in the plane transverse to the e^+ beam axis ($r\varphi$ plane), $\Delta\varphi > 135^\circ$, is applied at the trigger level. The signal inefficiency due to this trigger constraint is negligibly small because the final-state leptons tend to be back-to-back in the $r\varphi$ plane due to the kinematic properties of our selected final states, namely the strict p_t requirement on the χ_{c2} and the small mass difference between the χ_{c2} and J/ψ . The events from the $J/\psi \rightarrow e^+e^-$ mode are efficiently triggered by a total energy trigger derived from the ECL with a threshold set at 1.0 GeV.

The main backgrounds are leptonic final states from QED processes such as $e^+e^- \rightarrow e^+e^-\ell^+\ell^-\gamma$. The E/p information, which is the ratio of the energy deposit in the ECL to the track's momentum, is used to identify the leptons

² Q^2 is defined as the negative of the invariant mass squared of a virtual incident photon. It is approximately equal to $|p_t|^2$ of the virtual photon with respect to the e^+e^- beam axis.

and eliminate small backgrounds that contain hadron tracks.

3 Event selection

The event selection criteria are as follows: (1) Exactly two oppositely charged tracks reconstructed by the CDC, where both tracks satisfy the following laboratory frame conditions: $-0.47 \leq \cos \theta \leq +0.82$, where θ is the polar angle; $p_t \geq 0.4$ GeV/ c ; $|dr| \leq 1$ cm, $|dz| \leq 3$ cm, where ($|dr|$, $|dz|$) are the cylindrical coordinates of the track's point of closest approach to the nominal collision point in the $r\phi$ plane; $|\Delta dz| \leq 1$ cm, where Δdz is the difference between the dz 's of the two tracks; and no other well reconstructed tracks with p_t higher than 0.1 GeV/ c . (2) The opening angle (α) of the two tracks satisfies $\cos \alpha > -0.997$. (3) There is just one electromagnetic cluster in the ECL with an energy $E_\gamma \geq 0.2$ GeV and isolated from the nearest charged track by an angle greater than 18° . (4) The scalar sum of the momenta of the two charged tracks is less than 6 GeV/ c , and the invariant mass of the two tracks is between 1.5 and 4.5 GeV/ c^2 . (5) The total energy deposited in the ECL is less than 6 GeV. (6) The absolute value of the total transverse momentum vector in the c.m. frame of the e^+e^- beams, $|\mathbf{p}_t^{*\text{tot}}| = |\mathbf{p}_t^{*+} + \mathbf{p}_t^{*-} + \mathbf{p}_t^{*\gamma}|$, is less than 0.15 GeV/ c , while that for the two tracks only, $|\mathbf{p}_t^{*+} + \mathbf{p}_t^{*-}|$, is larger than 0.10 GeV/ c , where \mathbf{p}_t^{*+} , \mathbf{p}_t^{*-} and $\mathbf{p}_t^{*\gamma}$ are measured transverse momentum vectors (defined as two-dimensional momentum vectors projected onto the plane perpendicular to the beam axis in the e^+e^- c.m. system) for the positive track, the negative track and the photon, respectively. (7) For electron pairs, both tracks are required to have $E/p \geq 0.8$; for muon pairs, both tracks are required to have $E/p \leq 0.4$.

Selection criterion (2) rejects cosmic-ray backgrounds. Criterion (6) rejects two-photonic lepton-pair production events with radiation from a recoil electron or with a fake photon, which tend to populate the region $|\mathbf{p}_t^{*+} + \mathbf{p}_t^{*-}| \approx 0$. The scatter plot in the $|\mathbf{p}_t^{*+} + \mathbf{p}_t^{*-}|$ - $|\mathbf{p}_t^{*\text{tot}}|$ plane before the application of requirement (6) is shown in Fig. 1(a), where two separate clusters of events at $|\mathbf{p}_t^{*+} + \mathbf{p}_t^{*-}| \approx 0$ and $|\mathbf{p}_t^{*\text{tot}}| \approx 0$ are apparent. The latter cluster corresponds to exclusive $\ell^+\ell^-\gamma$ final states produced by two-photon collisions. The distribution from the signal events obtained from the Monte Carlo (MC) simulation (described in Sect. 5) is shown in Fig. 1(b).

We correct the absolute momenta of detected electrons or positrons for bremsstrahlung in $e^+e^-\gamma$ event candidates. If photons of energy between 0.02 and 0.2 GeV are present within a cone of half-angle 3° around the electron direction, the energy of the most energetic photon in the cone is added to the absolute momentum of the track. This correction is also effective for partially compensating for the radiative-decay events of J/ψ , $J/\psi \rightarrow e^+e^-\gamma$.

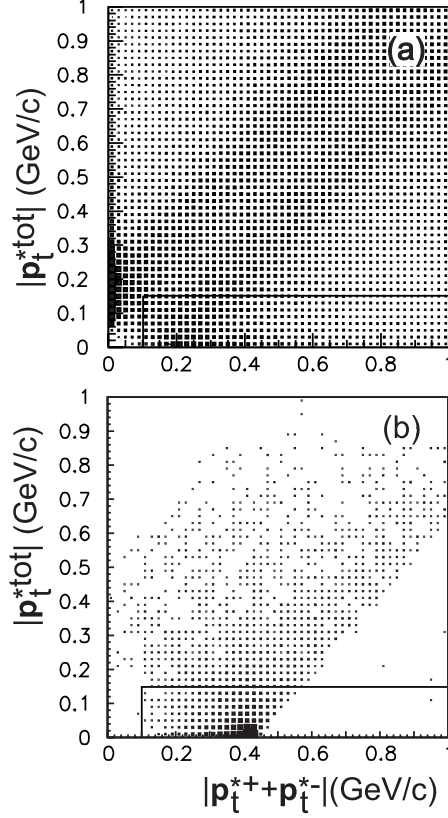


Fig. 1. Scatter plots for the absolute values of the two kinds of vector sums of the transverse momenta: the horizontal axis for the sum of the two charged particles, and the vertical axis of all three particles including the photon: (a) for real data and (b) for Monte Carlo events of the signal process. Straight lines show the selection requirements.

4 Derivation of the number of signal events

Figure 2 shows a scatter plot of the invariant mass of the two tracks (M_{+-}) versus the invariant-mass difference $\Delta M = M_{+-\gamma} - M_{+-}$ for the selected events, where $M_{+-\gamma}$ is the invariant mass of all three particles. A clear concentration is observed around $M_{+-} = 3.097 \text{ GeV}/c^2$ and $\Delta M = 0.459 \text{ GeV}/c^2$, the signal region for $\chi_{c2} \rightarrow \gamma J/\psi$.

The mass difference distribution is shown in Fig. 3(a) for the events falling within the J/ψ signal mass region $3.06 \leq M_{+-} \leq 3.13 \text{ GeV}/c^2$. After the final selection requirement for signal candidate events, $0.42 \leq \Delta M \leq 0.49 \text{ GeV}/c^2$, is applied, 176 events remain. Of these, 82 events have electron pairs and 94 have muon pairs. The contribution of χ_{c1} production, which would peak at $\Delta M = 0.42 \text{ GeV}/c^2$, is estimated to be less than one event, as expected from the suppression of spin-1 meson production in quasi-real two-photon collisions [9].

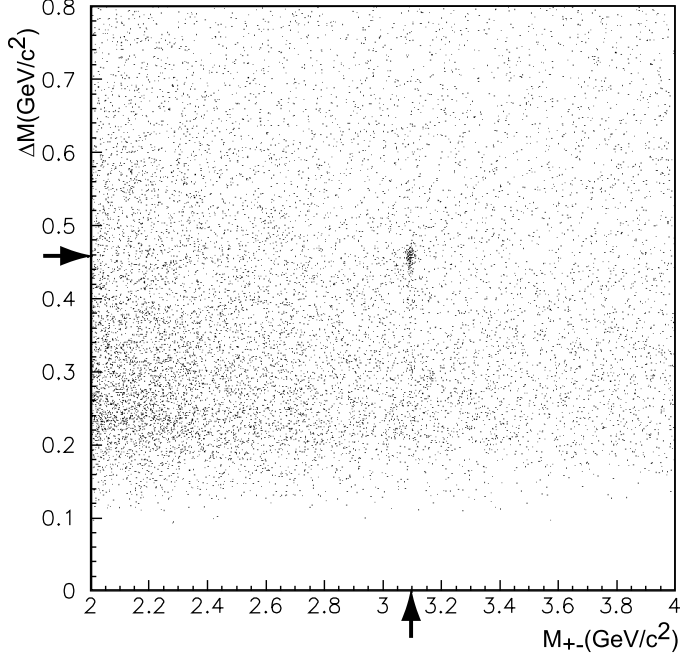


Fig. 2. Scatter plot of the invariant mass M_{+-} of the two-track system versus the mass difference $\Delta M = M_{+-\gamma} - M_{+-}$. The arrows indicate the nominal J/ψ mass and the ΔM value expected for $\chi_{c2} \rightarrow \gamma J/\psi$.

The ΔM distribution of events in the J/ψ -mass sideband regions ($2.65 < M_{+-} < 3.00 \text{ GeV}/c^2$ and $3.15 < M_{+-} < 3.50 \text{ GeV}/c^2$) is used to determine the background contribution (Fig. 3(b)). The ΔM distribution for J/ψ sideband events between $\Delta M = 0.15$ and $0.70 \text{ GeV}/c^2$ is fitted by an appropriate function³ to obtain the shape of the background distribution. We normalize this to the ΔM distribution of events in the J/ψ signal region, and determine the number of background events in the χ_{c2} signal region to be 40.0 ± 2.7 events. This normalization fit uses only data in the χ_{c2} sideband regions, $0.15 < \Delta M < 0.29 \text{ GeV}/c^2$ and $0.50 < \Delta M < 0.70 \text{ GeV}/c^2$. Since we expect 9 ± 7 events around $\Delta M = 0.32 \text{ GeV}/c^2$ from the χ_{c0} [3,7], we avoid that mass region. This expected χ_{c0} yield is consistent with the small excess of events seen near $\Delta M = 0.32 \text{ GeV}/c^2$ in Fig. 3(a). We determine the number of χ_{c2} signal events to be 136.0 ± 13.3 after subtracting the number of background events from the total in the signal region.

We find that the events in ΔM sideband regions are dominated by non- J/ψ backgrounds since the quantity and shape of the distribution agree with that of the J/ψ sideband. The 368 events in the $0.42 \leq \Delta M \leq 0.49 \text{ GeV}/c^2$ region in Fig. 3(b) consist of 176 electron pairs and 192 muon pairs. These backgrounds

³ We used the following empirical function for the fit of the background shape: $A(\Delta M - a)^{-b}/(1 + e^{-c(\Delta M - d)})$, where a , b , c and d are free parameters, and A the normalization parameter. We have confirmed that the change of the ΔM distribution shape is small at different M_{+-} points in the sideband region.

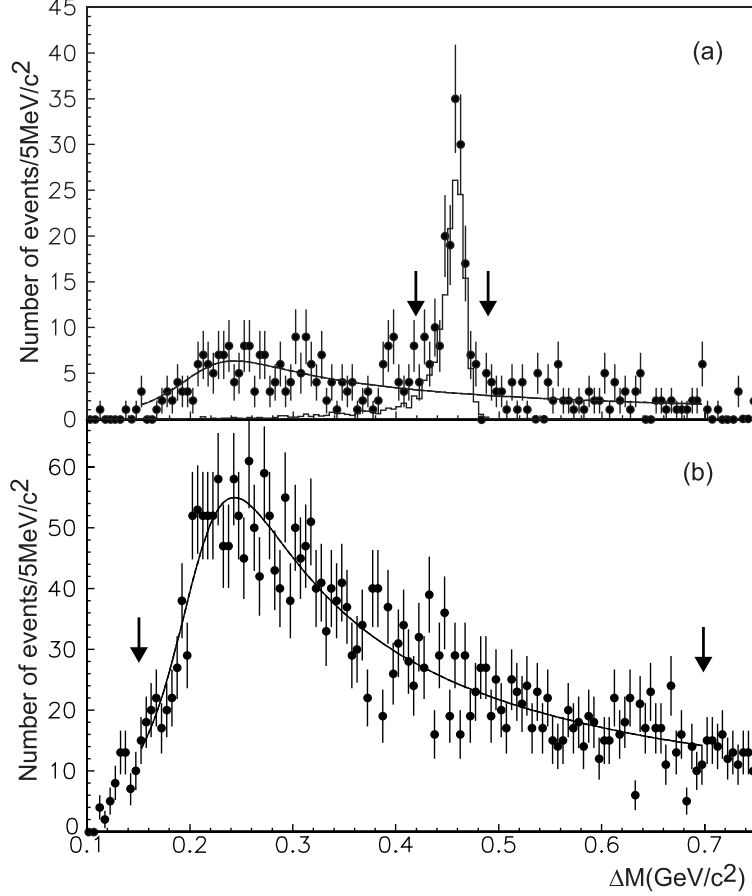


Fig. 3. The mass difference distributions for (a) events in the J/ψ -mass region (closed circles with error bars) and (b) sideband events. The curves in (a) and (b) indicate the results of the fits that are used to determine the background contribution in the signal region. The histogram in (a) shows the distribution of the signal MC events normalized to the observed signal. The arrows show the signal region (a) and the background control region (b).

are consistent with higher-order QED events such as $e^+e^- \rightarrow e^+e^-\ell^+\ell^-\gamma$, which would give comparable numbers of events with electron and muon pairs. In contrast, hadron production (in which pions would fake muons) would give primarily events containing muon pairs. Since a complete calculation of this process that takes interference effects into account is not available, we cannot estimate the background yield theoretically.

Figure 4 shows distributions for $\Delta\varphi$, $|\mathbf{p}_t^{*\text{tot}}|$, $|\cos\theta_\gamma^{+-\gamma}|$ and $\cos\theta_-^{+-}$ for the final candidate events, where $\Delta\varphi$ is the azimuthal angle difference between the two lepton's momenta in the laboratory frame, and $|\mathbf{p}_t^{*\text{tot}}|$ is the transverse momentum of the $\ell^+\ell^-\gamma$ system in the c.m. frame of the e^+e^- beams. $\theta_\gamma^{+-\gamma}$ and θ_-^{+-} are the polar angles of the photon in the $\ell^+\ell^-\gamma$ c.m. frame and of the negatively charged lepton in the $\ell^+\ell^-$ c.m. frame, respectively, where the polar angles are measured with respect to the incident e^- direction. The ex-

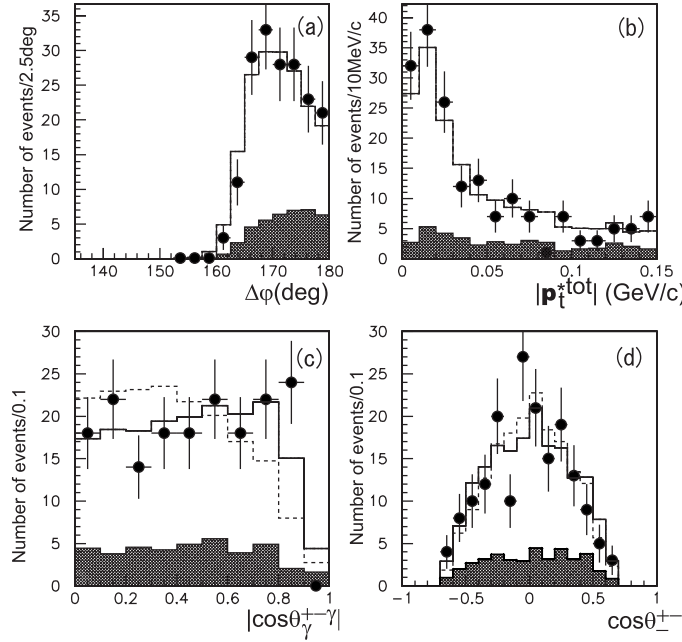


Fig. 4. Comparison of the final samples (closed circles with error bars, backgrounds included) with the sum of the signal MC events (open histogram) and estimated background contributions (hatched region) for: (a) $\Delta\phi$; (b) $|\mathbf{p}_t^{*tot}|$; (c) $|\cos\theta_{\gamma}^{+-}|$; and (d) $\cos\theta_{+-}^0$. There are no entries in the $\Delta\phi < 135^\circ$ region in (a). The dashed histograms in (c) and (d) show the distribution for the pure helicity=0 production case (see the text in Sect. 5).

perimental distributions are compared with the sum of the signal MC events, described in the next section, and the expected background contributions determined from the J/ψ sideband events, normalized to the observed numbers of events.

It is apparent from Fig. 4(a) that the final-state leptons have a back-to-back topology in the $r\phi$ plane, and the experimental data are consistent with the MC distribution. The data in Fig. 4(b) show a peak at very small p_t values ($|\mathbf{p}_t^{*tot}| < 30$ MeV/c) of the final-state system that is a typical feature of exclusive production in two-photon collisions; the data are in good agreement with the MC prediction. The distribution for sideband events has a less prominent concentration near $|\mathbf{p}_t^{*tot}| = 0$. In the angular distributions of Figs. 4(c) and 4(d), the data are consistent with the MC.

5 Monte Carlo calculations

We used Monte Carlo (MC) simulated $e^+e^- \rightarrow e^+e^-\chi_{c2}$, $\chi_{c2} \rightarrow \gamma J/\psi$, $J/\psi \rightarrow \ell^+\ell^-$ ($\ell = e$ or μ) events to calculate the efficiency for the signal process. The TREPS MC program [10] is used for the event generation. The effects of J/ψ radiative decays are modeled with the PHOTOS [11] simulation code, which generates photon radiation from a final-state lepton generated by TREPS with a probability determined by a QED calculation. All of the final-state particles in the MC events are processed by the full detector simulation program.

We assume that the χ_{c2} decay to the $\gamma J/\psi$ final state is an $E1$ transition, since experimental observations indicate that this transition dominates the decay [12]. Since the helicity state of χ_{c2} produced in two-photon collisions is not known, we assume a pure $\lambda = 2$ state [13], where λ is the helicity of χ_{c2} with respect to the $\gamma\gamma$ -incident axis. The measurement of the polar-angle distribution of the photon shown in Fig. 4(c) can be used to evaluate the possible contribution from a $\lambda = 0$ component. The $\lambda = 2$ component produces a $\cos\theta_\gamma^{+-\gamma}$ distribution that is proportional to $[1 + \cos^2\theta_\gamma^{+-\gamma}]$, whereas the $\lambda = 0$ component is proportional to $[5 - 3\cos^2\theta_\gamma^{+-\gamma}]$. The dashed histograms in Figs. 4(c) and 4(d) show the expected distributions from the pure $\lambda = 0$ state. The present experimental $\cos\theta_\gamma^{+-\gamma}$ distribution has better agreement with a pure $\lambda = 2$ hypothesis ($\chi^2/dof = 12.0/9$) than that for pure $\lambda = 0$ ($\chi^2/dof = 45.0/9$), or any other mixture of the two helicity states. Here, each χ^2/dof is calculated from the $|\cos\theta_\gamma^{+-\gamma}|$ distribution divided into ten bins, where the total event number in the expected signal distribution is fixed to the number of observed signal events.

The trigger efficiency is experimentally determined using Bhabha and $\mu^+\mu^-$ events that are collected with two or more different redundant triggers, as described above in Sect. 2. We estimate the probability for the signal-process events that survive the selection criteria to pass the trigger conditions to be $(99 \pm 1)\%$ ($(94 \pm 3)\%$) for $ee\gamma$ ($\mu\mu\gamma$) events; and $(96 \pm 2)\%$ in average. This estimation agrees with the results of a trigger simulation that is applied to the signal MC events. The trigger efficiency is also confirmed by the experimental yield of two-photon lepton-pair events, $e^+e^- \rightarrow e^+e^-\ell^+\ell^-$, which agrees with the expectation from a QED calculation [14].

The ECL photon energy resolution was studied by comparing experimental and MC mass-difference distributions for $D^{*0} \rightarrow D^0\gamma$ decays in e^+e^- annihilation events. We find that the photon energy resolution is 1.3 times the MC prediction. The same tendency is confirmed in the $\chi_{c1} \rightarrow \gamma J/\psi$ samples from B -meson decays and $\eta \rightarrow \gamma\gamma$ samples from two-photon collisions. If we use a correspondingly wider ΔM distribution for the $\chi_{c2} \rightarrow \gamma J/\psi$, it decreases the efficiency of the ΔM selection by 3.8% from the MC-determined value.

We take this effect into account as a correction for the efficiency and assign a systematic error of the same size ($\pm 3.8\%$). We confirm that the observed position and width of the signal peak in the data are consistent with their expected values.

When the trigger effects and the difference between the data and MC photon energy resolutions are taken into account, the overall efficiency is found to be 6.6%. This is the average of the e^+e^- and $\mu^+\mu^-$ decay channels; the ratio of the efficiencies for the two lepton species is $ee/\mu\mu = 0.70 \pm 0.03$. The lower efficiency for e^+e^- is due to the occasional presence of extra high-energy photons from radiative J/ψ decays and electron bremsstrahlung. When the $ee/\mu\mu$ ratio for the background component determined from the J/ψ sideband events is taken into account, we expect the event yields in the final samples to have a ratio $ee/\mu\mu = 0.74 \pm 0.04$. This value is consistent with the observed ratio for the final experimental samples: 0.87 ± 0.13 .

The two-photon luminosity function is also calculated by the TREPS program [10]. For consistency, the same upper cutoff value of the photon Q^2 , $Q_{\max}^2 = 1.0 \text{ GeV}^2$, and the same vector-meson pole effect are used in the calculation of the luminosity function and in the event generation. The uncertainty in the luminosity function due to the vector-meson pole effect (we adopt the J/ψ mass) is small, about 2%, since we apply a strict $|\mathbf{p}_t^{\text{tot}}|$ requirement that is well below the mass scale of the vector mesons. The Q_{\max}^2 value does not affect the product of the luminosity function and the detection efficiency, since it is chosen to be large enough to cover the acceptance of our $|\mathbf{p}_t^{\text{tot}}|$ requirement. The value of the TREPS luminosity function is compared with that obtained from a full-diagram calculation of the $e^+e^- \rightarrow e^+e^-\mu^+\mu^-$ process [14] in the small $|\mathbf{p}_t^{\text{tot}}|$ region. From the difference of the two results, the systematic error for the luminosity function is estimated to be 5%, which includes ambiguities from the choice of the form factor and the finite $|\mathbf{p}_t^{\text{tot}}|$ requirement.

6 Results and discussion

The two-photon decay width of the χ_{c2} is related to the signal event yield as

$$\begin{aligned} \frac{\text{Yield}}{\int \mathcal{L} dt} &= 20\pi^2 \frac{L_{\gamma\gamma}(m_{\chi_{c2}})\eta}{(c/\hbar)^2 m_{\chi_{c2}}^2} \Gamma_{\gamma\gamma}(\chi_{c2}) \mathcal{B}(\chi_{c2} \rightarrow \gamma J/\psi) \mathcal{B}(J/\psi \rightarrow \ell^+ \ell^-) \\ &= (0.309 \text{ fb/eV}) \times \Gamma_{\gamma\gamma}(\chi_{c2}) \mathcal{B}(\chi_{c2} \rightarrow \gamma J/\psi) \mathcal{B}(J/\psi \rightarrow \ell^+ \ell^-), \end{aligned}$$

where $\int \mathcal{L} dt$ is the integrated luminosity, η is the efficiency, $m_{\chi_{c2}} (= 3.556 \text{ GeV}/c^2)$ is the χ_{c2} mass and $L_{\gamma\gamma}(m_{\chi_{c2}}) (= 7.75 \times 10^{-4} \text{ GeV}^{-1})$ is the two-photon luminosity function at the χ_{c2} mass. The total width of χ_{c2} ($2.00 \pm 0.18 \text{ MeV}$ [3])

is much smaller than the present ΔM resolution (~ 9 MeV), and does not affect the present measurement.

The observed number of events, 136.0 ± 13.3 , implies the result $\Gamma_{\gamma\gamma}(\chi_{c2})\mathcal{B}(\chi_{c2} \rightarrow \gamma J/\psi)\mathcal{B}(J/\psi \rightarrow \ell^+\ell^-) = 13.5 \pm 1.3 \pm 1.1$ eV, where the first and second errors are statistical and systematic, respectively. This result corresponds to $\Gamma_{\gamma\gamma}(\chi_{c2})\mathcal{B}(\chi_{c2} \rightarrow \gamma J/\psi) = 114 \pm 11(stat.) \pm 9(syst.) \pm 2(B.R.)$ eV or $\Gamma_{\gamma\gamma}(\chi_{c2}) = 0.85 \pm 0.08(stat.) \pm 0.07(syst.) \pm 0.07(B.R.)$ keV, where the last errors correspond to the uncertainties of the branching ratios, $\mathcal{B}(\chi_{c2} \rightarrow \gamma J/\psi) = (13.5 \pm 1.1)\%$ and $\mathcal{B}(J/\psi \rightarrow \ell^+\ell^-) = (11.81 \pm 0.20)\%$ [3]. The systematic error has contributions from the trigger efficiency (2%), lepton identification efficiency (1.5%), photon detection efficiency (2%), inefficiency due to fake photons (less than 2%), J/ψ detection efficiency (2%), the ΔM cut efficiency (3.8%), background subtraction (2.3%), the luminosity function (5%) and other sources (less than 3%); these total 8% when combined in quadrature.

The error in the background subtraction is derived from the difference in signal yields in the ΔM signal region between the present method (counting the events in the signal region and subtracting the background contribution) and an alternative method in which the signal and the background components are simultaneously fitted to the ΔM distribution with all the shape and size parameters for the background and signal distributions allowed to float, with the Crystal-Ball line shape [15] used for the signal distribution. The error of the background normalization is also combined with this error.

The inefficiency due to an extra (fake) photon with $E > 0.2$ GeV is estimated to be less than 2% from an experimental study of the p_t -balanced $e^+e^- \rightarrow e^+e^-\mu^+\mu^-$ process.

The uncertainty due to the assumption that the χ_{c2} 's are produced in a pure $\lambda = 2$ state and decay via pure $E1$ transitions is not included in the systematic error. Production in the $\lambda = 0$ state at the 10% level would increase the detection efficiency by 7% and decrease the measured $\Gamma_{\gamma\gamma}(\chi_{c2})$ value by the same amount. Meanwhile, a small mixture of the $M2$ transitions as has been indicated by a measurement, $M2/E1 \simeq -0.093^{+0.039}_{-0.041} (= a_2(\chi_{c2}))$ in amplitude [12], gives only a 2% effect on the efficiency.

The Belle result for $\Gamma_{\gamma\gamma}(\chi_{c2})$ is compared with those from previous experiments [5–7] in Fig. 5. The present result has the smallest statistical and systematic errors of all the two-photon measurements and is consistent with the previous two-photon results. However, it is larger than the $p\bar{p}$ results. A review of the experimental results of various branching ratios of $\psi(2S)$ and χ_c decays [16] suggests that this discrepancy may come from incorrect values of $\mathcal{B}(\chi_{c2} \rightarrow \gamma J/\psi)$ and $\mathcal{B}(\chi_{c2} \rightarrow p\bar{p})$ that are used for the derivation of $\Gamma_{\gamma\gamma}(\chi_{c2})$ in these

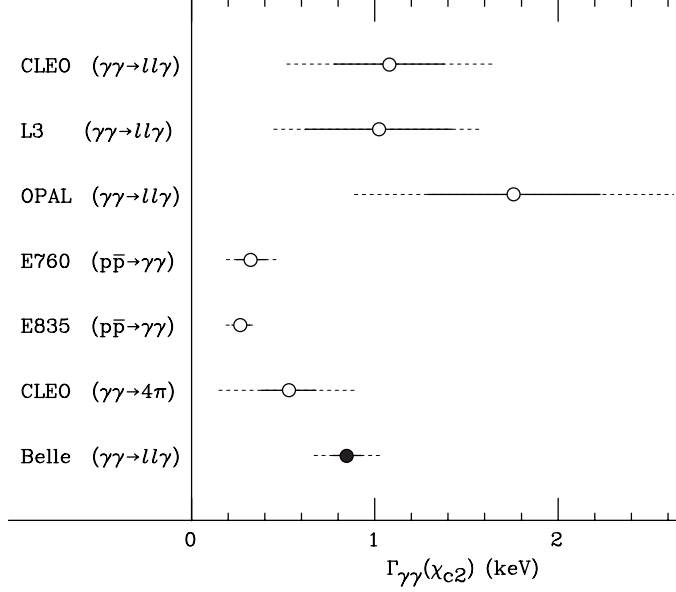


Fig. 5. Comparison of the Belle result for $\Gamma_{\gamma\gamma}(\chi_{c2})$ value with those from previous measurements[5–7]. The solid error bars show the statistical errors. The length of the dashed part in each error bar corresponds to the size of the systematic error, including the branching ratio uncertainty.

experiments.

7 Conclusion

We have measured χ_{c2} production from two-photon collisions with a 32.6 fb^{-1} data sample collected with the Belle detector at the KEKB e^+e^- collider, using the decay mode $\chi_{c2} \rightarrow \gamma J/\psi$, $J/\psi \rightarrow \ell^+\ell^-$. We find 136.0 ± 13.3 signal events after background subtraction. The observed polar-angle distributions of the photon and leptons are consistent with those expected from the production of χ_{c2} in the pure helicity 2 state. The product of the two-photon decay width of χ_{c2} and branching fractions, $\Gamma_{\gamma\gamma}(\chi_{c2})\mathcal{B}(\chi_{c2} \rightarrow \gamma J/\psi)\mathcal{B}(J/\psi \rightarrow \ell^+\ell^-) = 13.5 \pm 1.3(stat.) \pm 1.1(syst.) \text{ eV}$, is obtained. This result corresponds to $\Gamma_{\gamma\gamma}(\chi_{c2}) = 0.85 \pm 0.08(stat.) \pm 0.07(syst.) \pm 0.07(B.R.) \text{ keV}$, where the product of the branching fractions, $\mathcal{B}(\chi_{c2} \rightarrow \gamma J/\psi)\mathcal{B}(J/\psi \rightarrow \ell^+\ell^-) = (1.59 \pm 0.13)\%$ [3] is used.

Acknowledgements

We wish to thank the KEKB accelerator group for the excellent operation of the KEKB accelerator. We acknowledge support from the Ministry of Education, Culture, Sports, Science, and Technology of Japan and the Japan Society for the Promotion of Science; the Australian Research Council and

the Australian Department of Industry, Science and Resources; the National Science Foundation of China under contract No. 10175071; the Department of Science and Technology of India; the BK21 program of the Ministry of Education of Korea and the CHEP SRC program of the Korea Science and Engineering Foundation; the Polish State Committee for Scientific Research under contract No. 2P03B 17017; the Ministry of Science and Technology of the Russian Federation; the Ministry of Education, Science and Sport of the Republic of Slovenia; the National Science Council and the Ministry of Education of Taiwan; and the U.S. Department of Energy.

References

- [1] C. R. Münz, Nucl. Phys. A609 (1996) 364; H.-W. Huang, C.-F. Qiao, K.-T. Chao, Phys. Rev. D54 (1996) 2123.
- [2] W. Kwong, P. B. Mackenzie, R. Rosenfeld, J. L. Rosner, Phys. Rev. D37 (1988) 3210.
- [3] D. E. Groom et al., Eur. Phys. Jour. C15 (2000) 1, and 2001 off-year partial update for the 2002 edition available on the PDG WWW pages (URL: <http://pdg.lbl.gov/>)
- [4] G. T. Bodwin, E. Braaten, G. P. Lepage, Phys. Rev. D46 (1992) R1914.
- [5] TPC/Two-Gamma Collaboration, D. A. Bauer et al., Phys. Lett. B302 (1993) 345; CLEO Collaboration, J. Dominick et al., Phys. Rev. D50 (1994) 4265; OPAL Collaboration, K. Ackerstaff, Phys. Lett. B439 (1998) 197; L3 Collaboration, M. Acciarri et al., Phys. Lett. B453 (1999) 73.
- [6] E760 Collaboration, T. A. Armstrong et al., Phys. Rev. Lett. 70 (1993) 2988; E835 Collaboration, M. Ambrogiani et al., Phys. Rev. D62 (2000) 052002.
- [7] CLEO Collaboration, B. I. Eisenstein et al., Phys. Rev. Lett. 87 (2001) 061801.
- [8] Belle Collaboration, A. Abashian et al., Nucl. Instr. Meth. A479 (2002) 117.
- [9] G. A. Schuler, F. A. Berends, R. van Gulik, Nucl. Phys. B523 (1998) 423.
- [10] S. Uehara, KEK Report 96-11 (1996).
- [11] E. Barberio and Z. Was, Comput. Phys. Commun. 79 (1994) 291.
- [12] E835 Collaboration, M. Ambrogiani et al., Phys. Rev. D65 (2002) 052002; E760 Collaboration, T. A. Armstrong et al., Phys. Rev. D48 (1993) 3037; M. Oreglia et al., Phys. Rev. D25 (1982) 2259; L. S. Brown and R. N. Cahn, Phys. Rev. D13 (1976) 1195.
- [13] M. Poppe, Intern. Jour. Mod. Phys. A1 (1986) 545; H. Krasemann, J. A. M. Vermaseren, Nucl. Phys. B184 (1981) 269.

- [14] F. A. Berends, P. H. Daverveldt and R. Kleiss, Nucl. Phys. B253 (1985) 441;
F. A. Berends, P. H. Daverveldt and R. Kleiss, Comput. Phys. Commun. 40
(1986) 285.
- [15] T. Skwarnicki, Ph.D. Thesis, Institute for Nuclear Physics, Krakow 1986; DESY
Internal Report, DESY F31-86-02 (1986).
- [16] C. Patrignani, Phys. Rev. D64 (2001) 034017.